Progress In Electromagnetics Research B, Vol. 28, 325–350, 2011

GENETIC ALGORITHM APPROACH AND EXPERIMENTAL CONFIRMATION OF A LASER-BASED DIAGNOSTIC TECHNIQUE FOR THE LOCAL THERMAL TURBULENCE IN A HOT WIND TUNNEL JET

E. Pemha

Applied Mechanics Laboratory
Faculty of Science
University of Yaoundé I, P. O. Box 7389 Yaoundé, Cameroon

E. Ngo Nyobe

Department of Mathematics and Physical Science
Advanced National School of Engineering
University of Yaoundé I, P. O. Box 8390 Yaoundé, Cameroon

Abstract—This paper is devoted to a laser-based diagnostic technique described as a method for solving an applied inverse problem in turbulent media using laser beam propagation. This problem consists of extracting local information about temperature fluctuations inside a hot turbulent jet of air, from the luminous photodiode trace produced by a laser beam, after having traversed the jet. A genetic algorithm is implemented in order to calculate the optimized laser beam directions corresponding to the whole luminous trace. An approximated ray equation which is proved from the geometrical optics is solved numerically by using those directions and enables to determine the variance of temperature fluctuations along the whole path of the laser beam. A good agreement coming from the comparison between the results obtained and the published experimental data proves the validity of the method.

1. INTRODUCTION

Complex problems faced in the study of turbulent flows are caused mainly by the fact that the pressure, velocity and temperature are 3-dimensional random fields, which are governed by nonlinear and

Received 31 December 2010, Accepted 7 March 2011, Scheduled 14 March 2011
Corresponding author: E. Pemha (elkanaderbeau@yahoo.fr).

coupled partial differential equations (Navier-Stokes equations) whose difficulties to finding analytical solutions are well known. In addition, from the physical point of view, the mechanism of turbulence is particularly complex because of two factors: the vortex dynamic effects and the existence of intensive nonlinear interactions between turbulent structures of velocity, pressure, and temperature, highly irregular, covering a wide range of spatial and temporal scales, and then, creating an enormous amount of disorder.

Turbulence is a longstanding problem in fluid mechanics and many publications have already been devoted to its study [1–4]. But, there is no analytical or numerical solution, apart from a small number of cases which are always in need of models and simulations. Consequently, the experimental methods are inevitable and many scientists are making increasing use of optical techniques. The most effective optical methods are ones for which no measuring probe is introduced into the flow. In these optical techniques called diagnostic techniques, an electromagnetic wave usually characterized by a laser beam is sent into the turbulent flow studied, where fluctuations in temperature, pressure or density create random variations of the refractive index called optical turbulence. Under these circumstances, any attempt to solve the problem requires an understanding of the physics of optical wave propagation phenomenon through a turbulent medium.

Mastery of phenomena related to the propagation of a laser beam in an optical and thermal turbulence is also essential when trying to respond to the concerns encountered in a large number of technological applications based on the laser, such as medical diagnostic with laser [5], laser radar [6], laser probing of atmospheric properties [7], laser satellite communication and Earth-to-space communications [8], submarine detection [9], monitoring and remote sensing [10], laser weapons and laser defence missiles [11]... etc. Despite the great complexity of the fundamental problem which consists of analyzing the behavior of the light wave during its propagation through a random medium, various contributions have already been published.

Concerning theoretical studies, the general theory of propagation of a light wave in a turbulent medium is well explained by many authors [12–16], and numerical simulations coupled with models are also studied [17, 18].

With regard to experimental investigations, two goals are usually sought. The first is to develop techniques for measuring the effects caused by the turbulent environment on the optical characteristics of the laser beam during its spread [19–23]. The second objective which is an inverse problem of the previous one, involves design techniques for extracting local or global information on turbulence from the

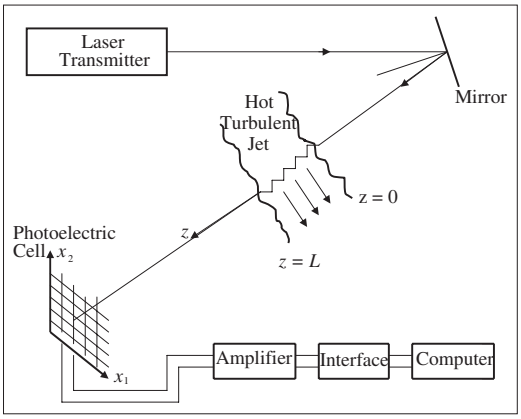

Figure 1. Experimental set-up [26, 29].

measurement of the statistical properties of the laser beam propagation in the medium [24–28]. The solution of the inverse problem explained in this work belongs to these laser beam diagnostic techniques, and the turbulent medium studied is a hot turbulent jet of air derived from the nozzle aperture of a wind tunnel.

This paper represents a continuation of our previous works [26–30]. About experiments, we consider the experimental set-up shown in Figure 1 and already used in our previous papers [26, 29]. A light beam (wavelength $\lambda_0 = 6328$ Å, initial diameter $a_0 = 0.8\,\text{mm}$) created from a 1 mW He-Ne laser, is passed through a heated plane air stream issued from a rectangular nozzle, before reaching a photoelectric cell placed outside the jet at a distance $d = 500\,\text{mm}$ from the jet border. Since the experimental results obtained by Gagnaire and Tailland [25] for the rms of temperature fluctuations, are used in order to validate the diagnostic technique that we have achieved in this paper, we need to carry out experiments by assuming Gagnaire's experimental conditions. So, the laser beam is placed in the zx_1 plane, at a distance $x_1 = 200\,\text{mm}$ from the plane of the nozzle aperture which has the same dimensions ($200\,\text{mm} \times 47\,\text{mm}$) as in [25]. At this position and along the whole path traversed by the laser ray, we have the same conditions as in [25], that is, the mean speed ($\overline{U} = 8\,\text{m/s}$) of the flow, the mean temperature ($\overline{T} = 50\,^\circ\text{C}$), and the rms of the temperature fluctuations ($\sqrt{\overline{\theta^2}} = 2.75\,^\circ\text{C}$) remain constants except in a short area at both borders of the stream. (See Section 6)

The theoretical part of this work is done under geometrical optics approximation; this holds if the conditions detailed in [27] are satisfied.

Since the incident radiation wavelength is $\lambda_0 = 6328$ Å, and the measurements [25] of the inner and outer scales of turbulence in the jet under study are $l_0 = 1\,\text{mm}$ and $L_0 = 10\,\text{mm}$, it is proved in our previous works [26–29] done with the same jet, that those conditions which allow the applicability of the geometrical optics approximation are satisfied.

The three Cartesian coordinates (z, x_1, x_2) are chosen such that the unperturbed direction of the laser beam is taken to be the z axis and the (x_1, x_2) plane is the cell plane. We use the measurements we have obtained for the probability density $W(x_1, x_2)$ of the position (x_1, x_2) of the laser beam impact centre on the photocell. It is useful to indicate that the measurements of these probabilities require to cross-rule the cell plane in 1600 small squares of the same size c, such that the discretized values of x_1 and x_2 are given by [26, 29]:

$$x_1(i) = x_{10} + i \cdot c, \quad i = 0, 1, \ldots, 40 \tag{1a}$$

$$x_2(j) = x_{20} + j \cdot c, \quad j = 0, 1, \ldots, 40 \tag{1b}$$

$$c = 5 \times 10^{-3}\,\text{cm} \tag{1c}$$

$$x_{10} = -0.15\,\text{cm} + 7c \tag{1d}$$

$$x_{20} = -0.15\,\text{cm} + 12c \tag{1e}$$

Although the results derived in [26–29] are satisfactory in terms of the order of magnitude of the values obtained, these measurements contain shortcomings that highlight a central issue. The problem resides in the fact that no local information about the turbulence of the jet studied can directly be deducted from these results. More specifically, the fundamental question that the analysis of these measurements leads to is: how the parameters of the light signal produced by the laser beam and collected on the photoelectric cell outside the jet, can be exploited to determine a local information about the thermal turbulence in the jet?

The objective of this work is to solve this inverse problem which consists of extracting local information about temperature fluctuations inside the heated turbulent jet, from the luminous photodiode trace produced by the laser beam, without introducing any measuring probe into the flow. Local variance of refractive index fluctuations which lead to local variance of temperature fluctuations are computed from an approximated laser beam equation, suitable for the problem under study. This equation is derived from the geometrical optics and enables to determine the local refractive index fluctuations if the directions of the laser beam are known. In order to calculate these directions, we consider and justify specific realisations of the optical turbulence in the jet, and a powerful optimization technique which includes a genetic algorithm is implemented.

For a better understanding of this work, this paper is organized as follows: Section 2 is devoted to the obtaining of an approximated ray equation for the problem under study. In Section 3, specific realisations of the optical turbulence in the jet are considered and justified. A spectral expansion for the directions of the laser beam is described in Section 4. In Section 5, the process of determining the directions of the laser beam by applying a genetic algorithm is explained in detail and the calculation method for the local variance of temperature fluctuations is presented. A rigorous measurement of the jet width for accurate numerical results is described in Section 6. Section 7 is devoted to practical considerations and to the results we have obtained. Conclusion is given in Section 8.

2. THE OBTAINING OF AN APPROXIMATED RAY EQUATION

The variance of the refractive index fluctuations is calculated from the integration of the following ray equation provided by the geometrical optics approximation:

$$\mathbf{grad}\, n = \frac{dn}{d\sigma}\tau + \frac{n}{R(\sigma)}\mathbf{v} \tag{2}$$

The quantity n represents the refractive index, τ and $\mathbf{v}$ are the unit vectors tangent and normal to the ray trajectory, connected by the well-known relation: $d\tau/d\sigma = \mathbf{v}/R(\sigma)$, in which $R(\sigma)$ is the curvature radius of the ray trajectory and σ the arc length of the ray curve. Usually, the above equation is used to determine the path of any light ray in a medium if the refractive index of this medium is known. In this paper, we are concerned with the inverse objective, that is, we consider laser beam paths and we seek the values of the refractive index along those paths, from the beam directions defined on the paths considered.

Since it is well known that the gradient component of the refractive index along the τ axis is defined as $dn/d\sigma$, the relation (2) shows that the main result given by the geometrical optics approximation is that the gradient component of the refractive index along the unit vector normal to the laser ray trajectory is equal to the quantity: $n/R(\sigma)$. Hence, we have to take only the projection of relation (2) along the $\mathbf{v}$ axis. Using the definition of the local incidence angle of the ray (see Figure 2), this gives the following equation:

$$|\mathbf{grad}\, n| \cos(\pi/2 - i) = |\mathbf{grad}\, n| \sin i = \frac{n}{R(\sigma)} \tag{3}$$

where i represents the local incidence angle of the ray, defined as $i=$ angle $(\tau, \mathbf{grad}\, n)$.

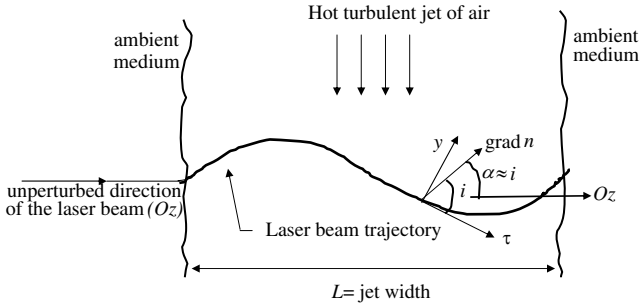

Figure 2. Local incidence angle i of the beam and refractive index gradient at any point M of the laser beam trajectory. $\alpha = \text{angle}\,(\tau_0, \text{grad}\, n) = \text{angle}(Oz, \text{grad}\, n) \approx i$.

Let τ_0, τ_1, and τ_2 be the Cartesian components of the vector τ along the directions (z, x_1, x_2). For the laser beam deviating very slightly from its initial incident direction Oz, the curvature radius is great at any point of the beam trajectory. Hence, the derivatives $\partial n/\partial x_1$ and $\partial n/\partial x_2$ are very small compared to $\partial n/\partial z$, and the transversal components τ_1 and τ_2 are very small compared to the longitudinal component τ_0.

It is possible to approximate the sine of the local incidence angle of the laser ray in order to exploit Equation (3). For this, let us write the equality between both forms of the scalar product $\tau \cdot \mathbf{grad}\, n$, that is:

$$\left(\frac{\partial n}{\partial z}\right)\tau_0 + \left(\frac{\partial n}{\partial x_1}\right)\tau_1 + \left(\frac{\partial n}{\partial x_2}\right)\tau_2 = |\mathbf{grad}\, n| \cos i \tag{4}$$

Using the approximation: $|\mathbf{grad}\, n| \approx |\partial n/\partial z|$, relation (4) leads to the approximated result: $(\frac{\partial n}{\partial z})\tau_0 \approx |\frac{\partial n}{\partial z}| \cos i$, which gives: $\cos i \approx \pm\tau_0$; that is: $\sin i \approx \sqrt{1-\tau_0^2}$. By replacing in relation (3), we obtain the following equation:

$$\left|\frac{\partial n}{\partial z}\right| = \frac{1}{\sqrt{1-\tau_0^2}}\frac{n}{R(\sigma)} \tag{5}$$

Knowing that the laser beam trajectory can be parameterized by the relations: $(z = z(\sigma),\ x_1 = x_1(\sigma),\ x_2 = x_2(\sigma))$, with $\tau_i = \tau_i(z(\sigma), x_1(\sigma), x_2(\sigma))$, (for $i = 0, 1, 2$), we replace in relation (5), the laser beam curvature $R^{-1}(\sigma)$ by the following definition:

$$\frac{1}{R(\sigma)} = \left(\left(\frac{d\tau_0}{d\sigma}\right)^2 + \left(\frac{d\tau_1}{d\sigma}\right)^2 + \left(\frac{d\tau_2}{d\sigma}\right)^2\right)^{1/2} \tag{6a}$$

in which the derivative $d\tau_i/d\sigma$ is given by:

$$\frac{d\tau_i}{d\sigma} = \tau_0 \left(\frac{\partial \tau_i}{\partial z}\right) + \tau_1 \left(\frac{\partial \tau_i}{\partial x_1}\right) + \tau_2 \left(\frac{\partial \tau_i}{\partial x_2}\right) \quad (\text{for} \quad i = 0, 1, 2) \tag{6b}$$

By applying the approximations $\partial/\partial x_1 \ll \partial/\partial z$ and $\partial/\partial x_2 \ll \partial/\partial z$, the formula of the laser beam curvature deriving from relations (6) can be simplified. Hence, relation (5) leads to the following equation:

$$\left|\frac{\partial N}{\partial z}\right| = \frac{1}{\sqrt{1-\tau_0^2}} \left(\left(\tau_0 \frac{\partial \tau_0}{\partial z}\right)^2 + \left(\tau_0 \frac{\partial \tau_1}{\partial z}\right)^2 + \left(\tau_0 \frac{\partial \tau_2}{\partial z}\right)^2\right)^{1/2} \tag{7}$$

$$\text{with :} \quad N = \text{Log}\,(n)$$

For solving the above equation, one needs to calculate the laser beam curvature $C(z, x_1, x_2)$ defined as the right hand side of this equation. If the azimuthal and polar angles (θ, ϕ) of the laser beam direction are known from any suitable modelling (see Section 3), the quantity $C(z, x_1, x_2)$ can be computed by applying the following relations:

$$\tau_0 = \sin\theta \cos\phi \tag{8a}$$

$$\tau_1 = \sin\theta \sin\phi \tag{8b}$$

$$\tau_2 = \cos\theta \tag{8c}$$

and:

$$\frac{\partial \tau_0}{\partial z} = \left(\frac{\partial \theta}{\partial z}\right) \cos\theta \cos\phi - \left(\frac{\partial \phi}{\partial z}\right) \sin\theta \sin\phi \tag{9a}$$

$$\frac{\partial \tau_1}{\partial z} = \left(\frac{\partial \theta}{\partial z}\right) \cos\theta \sin\phi + \left(\frac{\partial \phi}{\partial z}\right) \sin\theta \cos\phi \tag{9b}$$

$$\frac{\partial \tau_2}{\partial z} = -\left(\frac{\partial \theta}{\partial z}\right) \sin\theta \tag{9c}$$

This gives the following equivalent form for the Equation (7):

$$\left|\frac{\partial(\text{Log}\, n)}{\partial z}\right| = \frac{\sin\theta \cos\phi}{\sqrt{1-\sin^2\theta \cos^2\phi}} \left(\left(\frac{\partial \theta}{\partial z}\right)^2 + \sin^2\theta \left(\frac{\partial \phi}{\partial z}\right)^2\right)^{1/2} \tag{10}$$

Relation (10) is the approximated ray equation we have obtained for the problem under study.

3. A SIMPLIFIED NUMERICAL MODELLING FOR SOLVING THE APPROXIMATED RAY EQUATION

The problem stated by the determination of the refractive index n from Equation (10) can be solved as a Cauchy problem which normally

needs only a given initial condition at the entering plane $z = 0$. But, this solution must also verify the boundary condition at the outlet plane $z = L$. Hence, the fact that the first-order partial differential Equation (10) satisfies two dynamical conditions (that is more than one condition) leads to conclusion that the refractive index field should satisfy unknown mathematical conditions which do not depend on Equation (10). For this, we have to join to this equation a consistent numerical modeling which governs this field in the turbulent jet considered.

Since the temperature in the ambient medium is less than the temperature of the jet at the entrance of the laser beam, we can conclude, from the Dale-Gladstone law [13] that the refractive index decreases after entering the jet. That is, the gradient of the refractive index is negative in the vicinity of this border. In addition, we must take into account the fact that the thermodynamic conditions (temperature, pressure, specific mass, ...) are nearly identical in both ambient media located on both sides of the two plane jet borders $z = 0$ and $z = L$. This leads to conclusion that the boundary conditions for the refractive index are symmetrical with respect to the median jet plane $z = L/2$, that is:

$$N(z = 0, x_1, x_2) = N(z = L, x_1, x_2) \tag{11}$$

This condition is equivalent to the following relation:

$$\int_0^L \frac{\partial N}{\partial z} dz = 0 \tag{12}$$

From relation (12), we conclude that for all realisations of the turbulence in the jet, the gradient of the refractive index logarithm $\partial N/\partial z$ cancels in the interval $[0,\ L]$.

For simplifying the problem, let us consider the realisations of the jet turbulence for which the quantity $\partial N/\partial z$ cancels only at the point $(z = L/2, x_1, x_2)$, that is, it undergoes a negative symmetry at that point for any couple (x_1, x_2). Hence, we assume that the sign of the refractive index gradient remains unchanged in each regions of the jet limited as follows: $0 \leq z \leq L/2$ and $L/2 \leq z \leq L$. Consequently, from the above considerations, we can conclude that the gradient of the refractive index logarithm and the laser beam curvature C, satisfy the following relations:

$$\frac{\partial N}{\partial z} = -C(z, x_1, x_2) \quad \text{if} \quad 0 < z \leq L/2 \tag{13a}$$

$$\frac{\partial N}{\partial z}(z, x_1, x_2) = -\frac{\partial N}{\partial z}(L - z, x_1, x_2) \quad \text{if} \quad L/2 \leq z < L \tag{13b}$$

$$\frac{\partial N}{\partial z}\left(z=\frac{L}{2},x_1,x_2\right)=0 \tag{13c}$$

$$C\left(z=\frac{L}{2},x_1,x_2\right)=0 \tag{13d}$$

with:

$$C(z,x_1,\,x_2)=\frac{\sin\theta\cos\phi}{\sqrt{1-\sin^2\theta\cos^2\phi}}\left(\left(\frac{\partial\theta}{\partial z}\right)^2+\sin^2\theta\left(\frac{\partial\phi}{\partial z}\right)^2\right)^{1/2} \tag{14}$$

4. SPECTRAL EXPANSION FOR THE PROPAGATION DIRECTION OF THE LASER BEAM IN THE TURBULENT JET

In our previous works [26, 27, 29], it has been assumed that the random values of ϕ and θ depend only on the position of the laser beam impact centre on the photoelectric cell. This hypothesis is not realistic because it describes the laser beam diffusion process in the jet as a cone-shaped-diffusion-process in which the vertex is the laser beam entering point into the jet and the base being the laser beam luminous trace on the cell.

More recently [27], we have proposed laws in which the angles (θ,ϕ) of the laser beam direction vary as the spectral Fourier series expansion judiciously defined in terms of the propagation distance $\approx z$. In order to be suitable and realistic, these laws need to take into account the unperturbed direction $(\theta=\pi/2,\phi=0)$ of the laser beam and some reference directions $(\phi_L(x_1,x_2),\theta_L(x_1,x_2))$ suitably defined. We have written these laws as follows [27]:

$$\phi(z,x_1,\,x_2)=\phi_L(x_1,x_2)\left[1-\alpha\sum_{n=0}^{N}\left(a_n\sin\left(2n\pi\frac{z}{L}\right)+b_n\cos\left(2n\pi\frac{z}{L}\right)\right)\right] \tag{15a}$$

$$\theta(z,x_1,\,x_2)=\frac{\pi}{2}+\left(\theta_L(x_1,x_2)-\frac{\pi}{2}\right)\left[1-\alpha\sum_{n=0}^{N}\left(c_n\sin\left(2n\pi\frac{z}{L}\right)+d_n\cos\left(2n\pi\frac{z}{L}\right)\right)\right] \tag{15b}$$

The role of the shape parameter α is explained in [27] and a reference direction is defined as the direction of the straight line connecting the laser beam entering point and the laser beam impact on the photocell situated at a distance d from the jet border. Hence, any given reference direction corresponds to the specific group of random

laser beam trajectories which connect the laser beam entry point and a given impact of the laser beam on the photocell. In addition, the deflection angle of the laser beam being small, the angles ϕ and θ of the beam direction at any point of its trajectory are nearly equal to the corresponding angles of the position vector at the same point. Under these circumstances, the discretized coordinates defined by the relations (1) are needed and the reference directions are defined by the following equations:

$$\phi_L(x_1, x_2) \approx \phi_L(x_1(i), x_2(j)) = \tan^{-1}\left(\frac{x_1(i)}{L+d}\right) \tag{16a}$$

$$\theta_L(x_1, x_2) \approx \theta_L(x_1(i), x_2(j)) = \cot^{-1}\left(\frac{x_2(j)}{\sqrt{x_1(i)^2+(L+d)^2}}\right) \tag{16b}$$

$$i = 0, 1, \ldots, 40 \quad \text{and} \quad j = 0, 1, \ldots, 40.$$

The Fourier coefficients defined in the relations (15) verify the following constraints:

$$\sum_{n=0}^{N} b_n \cos(2n\pi) = \sum_{n=0}^{N} d_n \cos(2n\pi) = 0 \tag{17}$$

deduced from the boundary conditions on the outlet plane $z = L$, that is:

$$\phi(z = L, x_1, x_2) = \phi_L(x_1, x_2) \tag{18a}$$

$$\theta(z = L, x_1, x_2) = \theta_L(x_1, x_2) \tag{18b}$$

In this paper, additional constraints for the spectral Fourier coefficients are found and added to the conditions (17) previously mentioned in [27]. In fact, by applying the condition (13d) proved from the simplified modelling in Section 3, relation (14) gives the following conditions:

$$\frac{\partial \phi}{\partial z}(z = L/2, x_1, x_2) = \frac{\partial \theta}{\partial z}(z = L/2, x_1, x_2) = 0 \tag{19}$$

Since the derivatives $\partial\phi/\partial z$ and $\partial\theta/\partial z$ can be derived from relations (15) as follows:

$$\frac{\partial \phi}{\partial z} = -\frac{2\pi\alpha}{L}\phi_L(x_1, x_2)\sum_{n=0}^{N} n\left(a_n \cos\left(2n\pi\frac{z}{L}\right) - b_n \sin\left(2n\pi\frac{z}{L}\right)\right) \tag{20a}$$

$$\frac{\partial \theta}{\partial z} = -\frac{2\pi\alpha}{L}\left(\theta_L(x_1, x_2) - \frac{\pi}{2}\right)\sum_{n=0}^{N} n\left(c_n \cos\left(2n\pi\frac{z}{L}\right) - d_n \sin\left(2n\pi\frac{z}{L}\right)\right) \tag{20b}$$

condition (19) leads to the following additional constraints for the spectral Fourier coefficients:

$$\sum_{n=0}^{N} na_n \cos(n\pi) = \sum_{n=0}^{N} nc_n \cos(n\pi) = 0 \tag{21}$$

5. DETERMINATION OF THE LASER BEAM DIRECTIONS BY APPLYING A GENETIC ALGORITHM OPTIMIZATION AND CALCULATION OF LOCAL TEMPERATURE FLUCTUATIONS

Let us consider the quantity $P(z, x_1, x_2)$ which denotes the theoretical probability density for the point (z, x_1, x_2) to be situated on the random laser beam trajectory in the turbulent jet. Since the laser beam deflections remain very small, this probability density is approximately equal to the probability density $Q(z, \phi, \theta)$ of the laser beam to have the direction (ϕ, θ) after going a distance $\sigma \approx z$ in the turbulent jet. By assuming the hypothesis of the Markov model process for the direction (ϕ, θ) of the laser beam, Alim et al. [30] have found that the analytical expression of $Q(z, \phi, \theta)$ is a series expansion of spherical harmonics $Y_k^{mc}(\theta, \phi) = P_k^m(\cos\theta)\cos(m\phi)$, written as follows:

$$Q(z,\phi,\theta) = \sum_{k=1}^{\infty} \sum_{\substack{m=1 \\ m=odd}}^{k} \frac{1}{4\pi}(2k+1)\frac{(k-m)!}{(k+m)!}P_k^m(0) \exp[-k(k+1)D_\mu z]Y_k^{mc}(\theta,\phi) \tag{22}$$

where P_k^m are the associated Legendre functions ($k = 1, 2, 3, \ldots$ and $m = 1, 3, 5, \ldots$ with $m \leq k$) and D_μ is the diffusion coefficient of the hot turbulent jet defined in [12, 26, 27].

After having found that the convergence of the series defined in Equation (22) is ensured for $k \geq 185$, the probabilities $Q(z = L, \phi, \theta) \approx P(z = L, x_1, x_2)$ are computed from this equation, for the values of ϕ and θ given by the spectral expansion in Equations (15). These results, which depend on the parameter α, the diffusion coefficient D_μ, and the Fourier coefficients, must be compared to the measurements $W(x_1, x_2)$ of the same probabilities performed by means of the experimental setup in Figure 1. For this, we define a cost function J which measures the quadratic difference between the two sets of values, that is:

$$J = \iint \left[P(z = L, x_1, x_2) - W(x_1, x_2)\right]^2 dx_1 dx_2 \tag{23}$$

and the aim we seek is the minimization of J.

The convergence of the two Fourier series defined in the relations (15) being ensured if the integer N is very great, we have to solve an optimization problem which includes a great number of parameters. This problem is well known as an inverse problem of the parameter estimation type [31]. The value of the diffusion coefficient of the jet considered, the optimized value α^*, and the optimized values (a_n^*), (b_n^*), (c_n^*), (d_n^*) of the spectral coefficients which lead to the optimized laser beam directions according to the relations (15), form the global minimum of the cost function. For minimizing J, we propose to use a genetic algorithm (GA). The GA approach is strongly recommended for solving this problem because the cost function J depends on a lot of parameters which are of different types (α, diffusion coefficient and Fourier spectral coefficients), and are related to J by an unknown link in which differentiability can not be assumed.

Algorithms based on genetic ideas with stochastic approach were first introduced by Holland [32] and then widely developed by Goldberg [33] and Deb [34]. They have successfully been applied in engineering electromagnetics [35–38], in mechanical engineering [39, 40], and been coupled with turbulent flows in earlier papers, notably in metallurgy and manufacturing processes [41–43]. A GA works with a population of candidate solutions which are called individuals. It initializes a sample population and this population changes over generations with an unchanged number of individuals. Each individual is represented by a code defined by a single string of characters called chromosomes. A positive fitness function F whose definition does not depend on generation enables to calculate at each generation, the fitness of the current individuals. Based on the genetic of the human beings evolution, that is, the evolution via the survival of the fittest, a new generation of new individuals is generated after the three genetic operators: selection, crossover and mutation [44, 45]. The new population is thus created and the whole process repeats. In the course of the process, crossovers and mutations are authorized to be performed into an individual string at given probabilities P_C and P_M respectively. Since mutation plays a secondary role in a simple GA, the condition $P_M \ll P_C$ must be satisfied.

We have implemented the GA for a great maximum number of generations which is arbitrarily chosen, and we expect that the GA convergence will be obtained before reaching the last generation. In this case, the GA then gives the best individual which is defined to be the global optimum of the problem. Decoding this optimum enables to find the value of the diffusion coefficient of the jet and to obtain the optimized directions of the laser beam. These directions are used for solving the approximated ray Equation (10) which leads to the values

of the local temperature fluctuations.

Let us explain the calculation method which enables to compute the local variance of temperature fluctuations. Any observation plane (z = constant) situated in the jet is cross-ruled according to the discretized coordinates defined in Equations (1). From Equation (10), the refractive index values are calculated at the points of the region located at the vicinity of the laser beam trajectory. The fluctuations μ of the refractive index can then be deduced for any discretized point situated in this region, using the following definition:

$$\mu(z, x_1(i), x_2(j)) = n(z, x_1(i), x_2(j)) - \overline{n}(z) \tag{24}$$

where $n(z, x_1(i), x_2(j))$ are the values of the refractive index representing the solution of the approximate ray equation with the simplified numerical modeling explained in Section 3, and $\overline{n}(z)$ denotes the mean value of the refractive index. Assuming that the jet air may be considered as a perfect gas, and using the Dale-Gladstone law, the $\overline{n}(z)$ values are calculated as follows:

$$\overline{n}(z) = 1 + \frac{aP_0}{\overline{T}(z)} \tag{25}$$

where $P_0 = 1000\,\text{mb}$ is the air pressure, $\overline{T}(z)$ represents the mean temperature and a is a parameter defined as: $a = G(\lambda)/r$; $G(\lambda)$ is the Dale-Gladstone constant depending on the radiation wavelength λ, r is a specific constant of the perfect gas. For the incident wavelength of the laser beam we have used ($\lambda_0 = 6328$ Å), the value of a is $79 \times 10^{-6}\,\text{K}{\cdot}\text{mb}^{-1}$.

After having computed the probabilities $P(z, x_1(i), x_2(j))$ of the laser beam to reach the point $(z, x_1(i), x_2(j))$, the above values of μ are then used and enable to obtain the values of the variance of the refractive index fluctuations as follows:

$$\overline{\mu^2}(z) = \sum_{l=0}^{40} \sum_{m=0}^{40} \mu^2(z, x_1(i), x_2(j)) P(z, x_1(i), x_2(j)) \tag{26}$$

The values of the variance of the temperature fluctuations θ are then computed, using the following relation derived from the Dale-Gladstone law for perfect gas:

$$\overline{\theta^2}(z) = \left(\frac{\overline{T}^2(z)}{aP_0} \right)^2 \overline{\mu^2}(z) \tag{27}$$

The above relation holds if the pressure fluctuations are neglected in the turbulent jet considered. In the course of experiments, we have verified that the laser beam trajectory remains rectilinear before heating the jet. This leads to conclusion that pressure fluctuations have no considerable effects in the jet under study.

6. DEFINITION OF THE INITIAL CONDITION FOR THE APPROXIMATED RAY EQUATION AND MEASUREMENT OF THE JET WIDTH FOR ACCURATE NUMERICAL CALCULATIONS

About the initial condition for solving Equation (10), we mention that the ambient temperature is equal to 20°C and the ambient medium is at rest in the course of experiments; therefore, the ambient medium does not contain any refractive index fluctuations. Then, assuming that the entering jet border is approximated by the plane $z = 0$, and using the Dale-Gladstone law for the mean value of the refractive index, which is then equal to the local refractive index, we obtain the initial refractive index condition:

$$n(z = 0, x_1, x_2) = 1 + \frac{aP_0}{T_0} = \overline{n(z = 0, x_1, x_2)} = n_0 \qquad (28)$$

where T_0 represents the temperature at the jet borders.

Since the ambient medium is at rest, and since the planes $z = 0$ and $z = L$ represent the separation planes between the jet and the ambient medium, it follows that the jet borders are defined as the jet planes for which temperature fluctuations and refractive index fluctuations remain equal to zero. The jet width L which is the distance

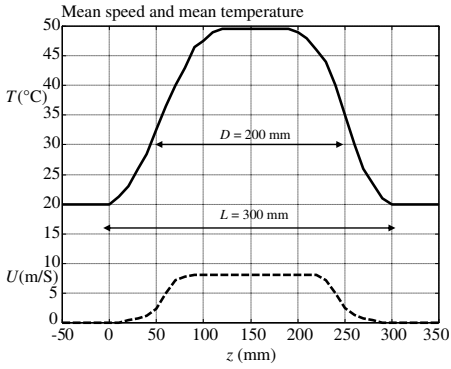

Figure 3. Definition of the jet width $L = 300\,\text{mm}$ as the distance between the planes $z = 0$ and $z = L$ such that $U(z = 0) = U(z = L) = 0$ and $T(z = 0) = T(z = L) =$ ambient temperature $= 20\,°\text{C}$. $D =$ width of the nozzle aperture $= 200\,\text{mm}$.

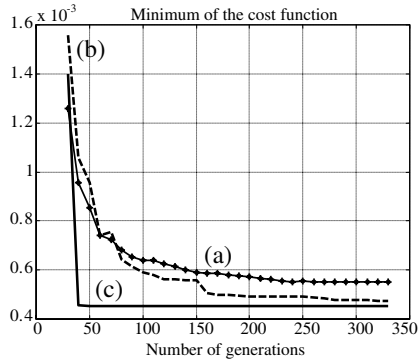

Figure 4. Convergence history of the GA optimization for three values of the population size: (a) 50; (b) 75; (c) 100.

between those borders must be carefully determined before solving Equation (10), in order to obtain accurate results. In our previous works [26–29], we have assumed, for simplicity, that L is equal to the width of the nozzle aperture = 200 mm. Since the inverse problem stated in this paper needs a rigorous determination of the jet width, we have to measure the mean speed U and the mean temperature T along the whole laser beam path. These measurements presented in Figure 3 enable to determine with more accuracy the positions of the planes $z = 0$ and $z = L$, and to deduce that the jet width L is equal to 300 mm. Figure 3 also shows that, along the whole path of the laser beam, the mean speed U and the mean temperature T remain constant and are equal to 8 m/s and 50 °C respectively, except at both borders of the heated jet. These results are the same as those obtained by Gagnaire and Tailland [25] along the same direction Oz in the turbulent jet.

7. PRACTICAL CONSIDERATIONS AND RESULTS

7.1. Practical Considerations Related to the Genetic Algorithm We Have Used

Some calculation tests made with the values of parameters properly chosen have shown that the order of magnitude of J is equal to 10^{-4}. We have then defined the fitness function F as: $F = 1.0 - 10J$. This definition ensures that F remains positive and the scaling factor applied to J makes significant discrepancies between the values of the function F. The selection technique we have used is tournament selection [44] with shuffling like in domino games. To improve convergence, we have applied the *elitist strategy* [45] which requires the fittest individual of each generation to survive into the next generation. In the course of GA calculation, one fittest individual was copied into the next generation.

The process of minimization of the function J includes a fundamental constraint due to the fact that the values of all optimized parameters must be chosen so that the computed probabilities remain situated between 0 and 1, for all planes of observation. For treating this constraint, a small value (10^{-6}) and a great value (100) are respectively assigned to the fitness function and the cost function, for any individual who violates this constraint. In order to make the process more efficient, an additional constraint is added to the problem: it is to ensure that the optimal values of the parameters may not correspond to the cases for which the laser beam undergoes a back-diffusion in the turbulent jet. For this, the component τ_0 of the unit vector tangent to the laser beam trajectory must remain positive. In the GA used, this

constraint is treated by assigning other arbitrary values to F and J, for individuals who violate this second constraint.

The area for the exploration of the optimized parameters should be properly chosen and large enough to avoid a priori exclusion of potential solutions. Moreover, it is desirable to work with large exploration areas which could include some "bad individuals" in order to create a diverse population; this helps to avoid premature convergence of the GA. In this regard, we find that it is sufficient to obtain at least one acceptable individual for a particular generation so that the GA subsequently produces acceptable individuals whose number is growing across generations. For the Fourier coefficients we have selected the same exploration area equal to $A_1 =]-1, +1[$. Concerning the parameter α, two requirements are met: on the one hand, the choice of small values for α could lead to a non realistic case corresponding to canceling the role of the Fourier series in Equations (15). On the other side, great values of α give values of ϕ and θ which could not be in the vicinity of the reference values ϕ_L and θ_L, and then, increase the risk of violating the constraints. After many tests, we have found that a suitable exploration area for the parameter α is the interval $A_2 =]-0.6, 0.6[$. Concerning the positive parameter D_μ, previous measurements [26, 27] suggest taking its order of magnitude equal to $10^{-9}\,\mathrm{m}^{-1}$. So, the exploration area we have taken for D_μ is the interval $A_3 = [1.0 \times 10^{-9}\,\mathrm{m}^{-1}, 10.0 \times 10^{-9}\,\mathrm{m}^{-1}]$.

For optimizing a given parameter r, we have used a binary code which needs to define discretized values of this parameter such that: $r_i = r_l + i(\Delta r)$ with: $i = 0, \ldots, N_r$ and $\Delta r = (r_u - r_l)/N_r$, r_l and r_u being the lower and upper values of r . So, there is a unique correspondence between each value r_i of a given parameter r and the discretization integer i such that coding r_i means coding i. For simplicity, we have adjusted the number of discretization values to a power of 2; this number is equal to $1024 = 2^{10}$, that is, 10 chromosomes per parameter. Since the total number of parameters which we have to optimize is equal to 406 (4×101 Fourier coefficients, α, D_μ) this gives a total number of chromosomes equal to 4060. By applying the constraint conditions found in Equations (17) and (21), the total number of Fourier coefficients is reduced to $404 - 4 = 400$ coefficients. So, we have coded each individual as a string of 4020 chromosomes.

The maximal number of generations arbitrarily defined is equal to 300 for any run. Initially, the number K of observation planes perpendicular to the x axis is chosen very large ($K = 800$) and the genetic algorithm is then implemented using random-site crossovers (rate = 0.70), genotypic mutations (rate = 0.02) and phenotypic mutations (rate = 0.04). In Figure 4, the convergence history of the

GA optimization is presented for three values of the population size (50, 75, 100). From the initial values $J = 12.56 \times 10^{-4}$, 15.58×10^{-4}, 13.98×10^{-4}, respectively used for these populations, the cost function is reduced to the minimum $J = 4.51 \times 10^{-4}$. For the population size = 100, the GA begins to converge after 252 generations, when the best individual for all subsequent generations, is obtained for the first time. The final results we have presented are obtained for the population size = 100. Altering the GA parameters according to Goldberg's recommendations [33] (Example: crossover rate = 0.60, rate of genotypic mutations = 0.03, rate of phenotypic mutations = 0.04), other groups of GA parameters have properly been taken for additional runs and we have found that the convergence process of the GA does not considerably change and that the best individual remains unchanged.

After having decoded the best individual given by the GA, we find that the value of the diffusion coefficient D_μ of the turbulent jet is $D_\mu = 2.18 \times 10^{-9}\,\mathrm{m}^{-1}$. Since the experimental value of D_μ deduced from the measurements of Gagnaire and Tailland [25] is $D_\mu = 2.20 \times 10^{-9}\,\mathrm{m}^{-1}$, we conclude that the value we have obtained in this work is more accurate than our previous result $D_\mu = 2.30 \times 10^{-9}\,\mathrm{m}^{-1}$ obtained by means of a GA and published in [27]. We also obtained from the decoded best individual the optimized values a_n^*, b_n^*, c_n^* and d_n^* of the Fourier coefficients. These values enable to compute the values of the non-dimensional angle functions F_ϕ and F_θ defined from relations (15) as follows:

$$F_\phi(z, x_1, x_2) = \frac{\phi_L(x_1, x_2) - \phi(z, x_1, x_2)}{\phi_L(x_1, x_2)} \tag{29a}$$

$$F_\theta(z, x_1, x_2) = \frac{(\theta_L(x_1, x_2) - \pi/2) - (\theta(z, x_1, x_2) - \pi/2)}{\theta_L(x_1, x_2) - \pi/2} \tag{29b}$$

In Figures 5 and 6, these values are plotted as function of the propagation distance z for a given (x_1, x_2). These curves show the irregular variations of the laser beam direction depending on the propagation distance, according to the simplified modelling we have described for the gradient of the refractive index logarithm.

7.2. Values of Probabilities of the Laser Beam Direction Computed from Equation (22) by Applying the Spectral Expansion of the Laser Beam Directions

For convergence requirements, the number N of data groups on the basis of which is made the spectral Fourier decomposition of the turbulent laser beam directions, is assumed to be equal to 100. The

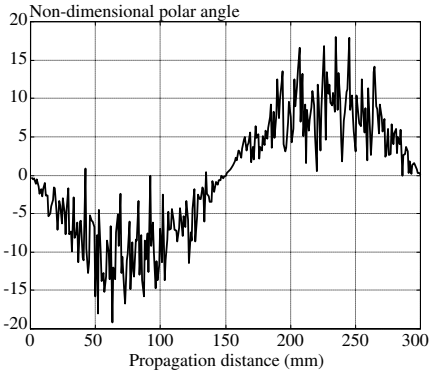

Figure 5. Quantity $F_\phi(z) = (\phi_L(x_1, x_2) - \phi(z, x_1, x_2, x))/\phi_L(x_1, x_2)$ as function of z.

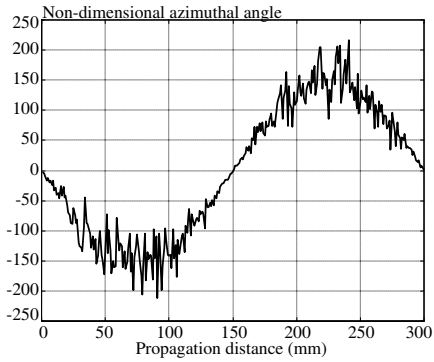

Figure 6. Quantity $F_\theta(z) = (\theta_L(x_1, x_2) - \theta(z, x_1, x_2,))/(\theta_L(x_1, x_2) - \pi/2)$ as function of z.

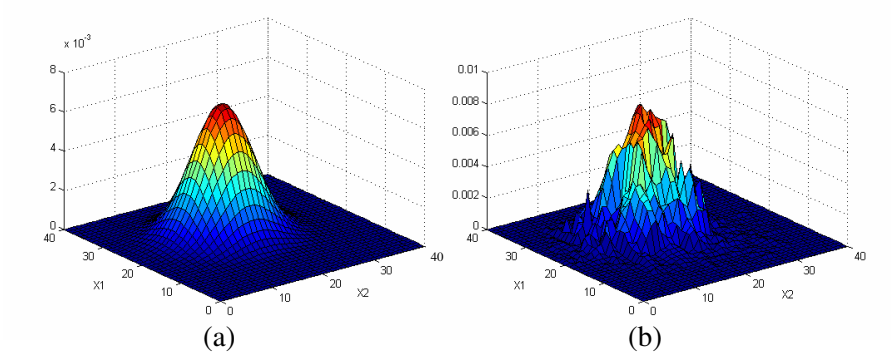

Figure 7. Probabilities of the laser beam impact positions on the photoelectric cell. (a) Numerical values obtained from the GA approach coupled with the Markovian model. (b) Experimental values [26, 29].

probabilities $P(z = L, x_1, x_2)$ of the beam impact positions on the cell are thus calculated from Equation (22) by using relations (15), when all the parameters of the problem take their optimal values. By comparing these probabilities plotted in Figure 7(a), with the experimental probabilities plotted in Figure 7(b), we find that the two results are in agreement. The match between the two sets of results appears much more when we compare the modeled and experimental forms of the same luminous trace produced by the laser beam on the photoelectric cell (Figure 8(a) and Figure 8(b)). This consistency is also reflected in Figures 9 and 10, which represent the marginal

probabilities (modelled and experimental) for the coordinates x_1 and x_2 of the beam impact position on the cell. By superimposing these marginal probability curves, we find an almost complete coincidence between modelled and experimental results.

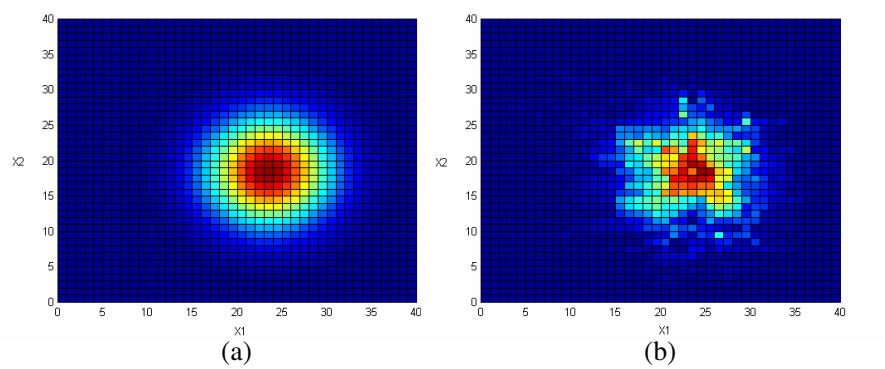

Figure 8. Luminous trace produced by the laser beam on the photoelectric cell. (a) Numerical values obtained from the GA approach coupled with the Markovian model. (b) Results derived from the experimental values [26, 29].

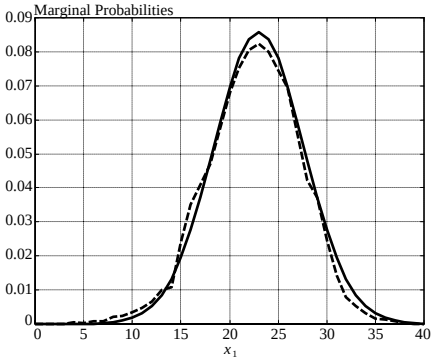

Figure 9. x_1 — coordinate marginal probabilities of the laser beam impact on the cell plane. Numerical values obtained from the GA approach coupled with the Markovian model (full curve). Results derived from the experimental values (dashed curve) [26, 29].

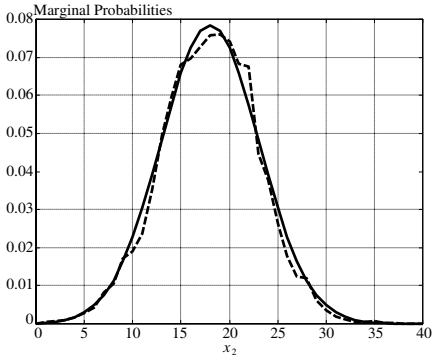

Figure 10. x_2 — coordinate marginal probabilities of the laser beam impact on the cell plane. Numerical values obtained from the GA approach coupled with the Markovian model (full curve). Results derived from the experimental values (dashed curve) [26, 29].

7.3. Calculation of the Refractive Index Gradient, Laser Beam Curvature, and rms of Temperature Fluctuations, by Using the Optimized Laser Beam Directions Derived from the Genetic Algorithm

After the above process, the GA parameters are retained constant and the optimized values of the Fourier coefficients are used for the calculation of the refractive index values, from the integration of Equation (10). For this, we have applied the well-known Simpson integration algorithm. So, let K_z be the number of discretized points situated along the z axis, in the interval $[0, L]$. Calculations are initially performed by using a great value of K_z ($K_z = 700$). We then study the effects of decreasing the number K_z in order to verify the convergence of the Simpson algorithm. These convergence tests enable us to find that convergence is ensured for the values of K_z greater than 265. By setting $K_z = 280$, the rest of our work is done.

The values we have then obtained for the non-dimensional refractive index gradient $L(\partial n/\partial z)$ are plotted in Figure 11, for a given (x_1, x_2). Figure 12 shows the non-dimensional values of the laser beam curvature, calculated according to the simplified numerical model. The refractive index values thus computed are used for determining the variance of refractive index fluctuations and that of temperature fluctuations, by applying the formulas (26) and (27). In Figure 13, the rms values of computed temperature fluctuations are compared to those measured by Gagnaire and Tailland [25], by means of a cold wire anemometer technique. We find a very satisfactory agreement which

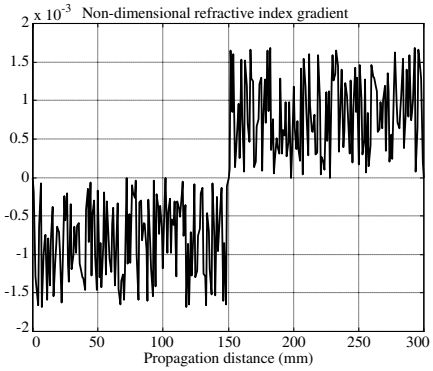

Figure 11. Non-dimensional Refractive index gradient $L(\partial n/\partial z)$ along the Oz direction.

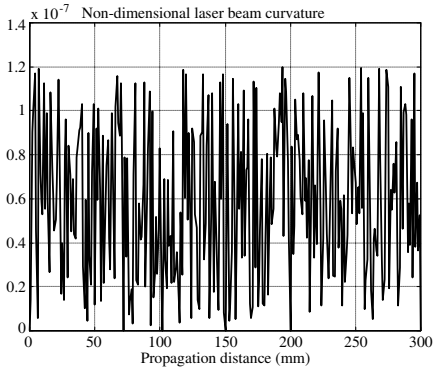

Figure 12. Non-dimensional laser beam curvature LC along the Oz direction.

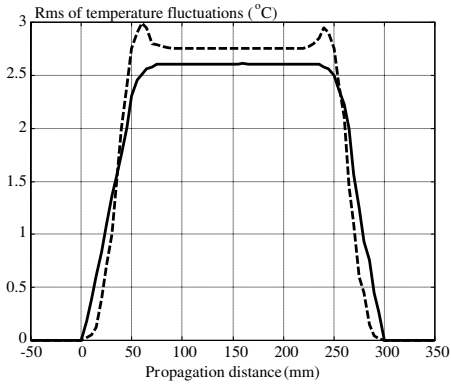

Figure 13. Computed rms of temperature fluctuations and Comparison with the experimental results: Experimental values (dashed curve) — Computed values (full curve).

is observed along the whole propagation distance of the laser beam.

In a very small area bounding the two borders of the jet, that is, the area defined as the influence zone of mixing between the ambient air and the hot turbulent jet, a slight difference between the above groups of results can be observed. More precisely, our calculation method is not able to highlight the two local maximums of the rms of temperature fluctuations observed in the experimental measurements [25], at both borders of the jet.

8. CONCLUSION

The importance of this work lies in one of the major challenges facing the scientific community of turbulence which is the design of techniques for turbulence diagnostics, that is, techniques which enable to extract local information about turbulence, without introducing any measurement probe into the turbulent medium. These techniques are the basis of many laser-based systems such as: medical diagnostic with laser, laser probing of atmospheric properties, laser satellite communication, Earth-to-space laser communications, laser radar, submarine detection, monitoring and remote sensing, laser weapons and laser defence missiles... etc.

In this paper, we have developed a robust method for solving an inverse problem which consists of determining the local temperature fluctuations in a hot turbulent jet of air, from the luminous trace produced by a laser beam on a photoelectric cell, after having traversed

the jet. The calculation procedure we have described shows that the above problem can be stated as an optimization problem of the parameter estimation type. The great number of parameters required by the problem recommends the use of a genetic algorithm which enables to determine the optimized laser beam directions.

An approximated ray equation governing the inverse problem is obtained and proved. Solving this equation is not easy because it appears to be a Cauchy problem which normally needs an initial condition, but it behaves in reality as a two-point-boundary-value-problem. This leads to conceive a consistent modeling for the behavior of the local refractive index gradient in the jet studied. The integration of that equation using the optimized laser beam directions enables to determine the rms of temperature fluctuations along the laser beam trajectory in the turbulent jet.

The good agreement between the results we have achieved and the published data obtained by means of the cold-wire anemometer technique proves the validity of the laser beam diagnostic technique explained in this paper. This suggests the possibility of using the above technique for the diagnostic of thermal turbulence in other flows, in particular those including combustion phenomena.

ACKNOWLEDGMENT

The authors would like to thank Emeritus Professors Bernard GAY and Jacques SAU of the University of Lyon I, for the collaboration between the Applied Mechanics Laboratory of the University of Yaoundé I (Cameroon) and the Laboratory of Fluid Mechanics of the University of Lyon I (France).

REFERENCES

1. Kolmogorov, A. N., "The local structure of turbulence in incompressible viscous fluids for very large Reynolds numbers," *Turbulence Classic Papers on Statistical Theory*, S. K. Friedlander and L. Topper (eds.), 151–155, Wiley-Interscience, New-York, 1961.
2. Frish, U., *Turbulence: The Legacy of A. N. Kolmogorov*, Cambridge University Press, Cambridge, 1995.
3. Tennekes, H. and J. L. Lumley, *A First Course in Turbulence*, MIT Press, Cambridge, 1971.
4. Monin, S. A. and A. M. Yaglom, *Statistical Fluid Mechanics: Mechanics of Turbulence (1 & 2)*, MIT Press, Cambridge, 1975.

5. O'Halloran, M., M. Glavin, and E. Jones, "Rotating antenna microwave imaging system for breast cancer detection," *Progress In Electromagnetics Research*, Vol. 107, 203–217, 2010.
6. Alexopoulos, A., "Effect of atmospheric propagation in RCS predictions," *Progress In Electromagnetics Research*, Vol. 101, 277–290, 2010.
7. Genc, O., M. Bayrak, and E. Yaldiz, "Analysis of the effects of GSM bands to the electromagnetic pollution in the RF spectrum," *Progress In Electromagnetics Research*, Vol. 101, 17–32, 2010.
8. Bukhsh, W. A., B. L. G. Jonsson, and P. Persson, "Element position perturbation for a narrow spot beam with applications in satellite communications antennas," *Progress In Electromagnetics Research*, Vol. 104, 283–295, 2010.
9. Wang, C. J., B. Y. Wen, Z. G. Ma, W. D. Yan, and X. J. Huang, "Measurement of river surface currents with UHF FMCM radar systems," *Journal of Electromagnetics Waves and Applications*, Vol. 21, No. 3, 375–386, 2007.
10. Liang, D., P. Xu, L. Tsang, Z. Gui, and K.-S. Chen, "Electromagnetic scattering by rough surfaces with large heights and slopes with applications in microwave remote sensing of rough surface over layered media," *Progress In Electromagnetics Research*, Vol. 95, 199–218, 2009.
11. Titterton, D. H., "A review of optical countermeasures," *Proceedings SPIE Conference on Technologies for Optical Countermeasures*, Vol. 5615, 1–15, London, 2004.
12. Chernov, L. A., *Wave Propagation in a Random Medium*, McGraw-Hill, New-York, 1960.
13. Tatarskii, V. I., *Wave Propagation in a Turbulent Medium*, McGraw-Hill, New-York, 1961.
14. Martini, A., L. Marchi, M. Franceschitti, and A. Massa, "Stochastic ray propagation in stratified random lattices — comparative assessment of two mathematical approaches," *Progress In Electromagnetics Research*, Vol. 71, 159–171, 2007.
15. Ishimaru, A., *Wave Propagation and Scattering in Random Media (1 & 2)*, Academic Press, New-York, 1978.
16. Clifford, S. F., "The classical theory of wave propagation in a turbulent medium," *Laser Beam Propagation in the Atmosphere*, J. W. Strohbehn (ed.), 9–43, Topics in Applied Physics (25), Springer-Verlag, 1978.
17. Li, Y. and H. Ling, "Numerical modelling and mechanism analysis of VHF wave propagation in forested environments using the

equivalent slab model," *Progress In Electromagnetics Research*, Vol. 91, 17–34, 2009.

18. Tromeur, E., E. Garnier, P. Sagaut, and C. Basdevant, "Large eddy simulations of aero-optical effects in a turbulent boundary layer," *Journal of Turbulence*, Vol. 4, No. 5, 1–22, 2003.
19. Hona, J., E. Ngo Nyobe, and E. Pemha, "Experimental technique using interference pattern for measuring directional fluctuations of a laser beam created by a strong thermal turbulence," *Progress In Electromagnetics Research*, Vol. 84, 289–306, 2008.
20. Consortini, A. and K. A. O'Donnell, "Beam wandering of thin parallel beams through atmospheric turbulence," *Waves in Random Media*, Vol. 3, S11–S28, 1991.
21. Wei, H.-Y., Z.-S. Wu, and Q. Ma, "Log-amplitude variance of laser beam propagation on the slant path through the turbulent atmosphere," *Progress In Electromagnetics Research*, Vol. 108, 277–291, 2010.
22. Hanada, T., K. Fujisaki, and M. Tateiba, "Theoretical analysis of a bit error rate for satellite communications in ka-band under atmospheric turbulence given by Kolmogorov model," *Journal of Electromagnetic Waves and Applications*, Vol. 23, Nos. 11–12, 1515–1524, 2009.
23. Ivanova, I. V., D. I. Dimitriev, and V. S. Sirazetdinov, "Probability density of intensity fluctuations for laser beams disturbed by turbulent aero-engine exhaust," *Proceedings of SPIE*, 6594, 2007.
24. Innocenti, C. and A. Consortini, "Refractive index gradient of the atmosphere at near ground levels," *Journal of Modern Optics*, Vol. 52, No. 5, 671–689, 2005.
25. Gagnaire, A. and A. Tailland, "Interferometrical setup for the study of thermic turbulence in a plane airstream," *Proceedings of SPIE*, Vol. 138, 69–73, 1977.
26. Pemha, E., B. Gay, and A. Tailland, "Measurement of the diffusion coefficient in a heated plane airstream," *Physics of Fluids*, Vol. 5, No. 6, 1289–1295, 1993.
27. Ngo Nyobe, E. and E. Pemha, "Shape optimization using genetic algorithms and laser beam propagation for the determination of the diffusion coefficient in a hot turbulent jet of air," *Progress In Electromagnetics Research B*, Vol. 4, 211–221, 2008.
28. Benzirar, M., E. Pemha, A. Tailland, and B. Gay, "About a new modelling of an optical technique for measuring local turbulent temperature fluctuations inside a hot free-plane jet

of air," *Experimental Heat Transfer, Fluid Mechanics and Thermodynamics*, M. D. Kelleher, R. K. Shah, K. R. Sreenivasan, and Y. Joshi (eds.), 1615–1619, Elsevier Science Publishers B. V., New-York, 1993.

29. Ngo Nyobe, E. and E. Pemha, "Propagation of a laser beam through a plane and free turbulent heated air flow: Determination of the stochastic characteristics of the laser beam random direction and some experimental results," *Progress In Electromagnetics Research*, Vol. 53, 31–53, 2005.
30. Alim, A., E. Ngo Nyobe, and E. Pemha, "Theoretical prediction and experimental validation of the angle-of-arrival probability density of a laser beam in a strong plane-flame turbulence," *Optics Communications*, Vol. 283, No. 9, 1859–1964, 2010.
31. Beck, J. V. and K. J. Arnold, *Parameter Estimation in Engineering and Science*, John Wiley and Sons, New-York, 1977.
32. Holland, J. H., *Adaptation in Natural and Artificial Systems*, University of Michigan Press, Ann Arbor, 1975
33. Goldberg, D. E., *Genetic Algorithms in Search, Optimization and Machine Learning*, Addison-Wesley, Reading, MA, 1989.
34. Deb, K., *Multi-objective Optimization Using Evolutionary Algorithms*, John Wiley and Sons, New-York, 2001
35. Tokan, F. and F. Gunes, "The multi-objective optimization of non-uniform linear phased arrays using the genetic algorithm," *Progress In Electromagnetics Research B*, Vol. 17, 135–151, 2009
36. Zhang, Y.-J., S.-X. Gong, and Y.-X. Xu, "Radiation pattern synthesis for arrays of conformal antennas mounted on an irregular curved surface using modified genetic algorithms," *Journal of Electromagnetic Waves and Applications*, Vol. 23, No. 10, 1255–1264, 2009.
37. Panduro, M. A., C. A. Brizuela, L. I. Balderas, and D. A. Acosta, "A comparison of genetic algorithms, particle swarm optimization and the differential evolution method for design of scannable circular antenna arrays," *Progress In Electromagnetics Research B*, Vol. 13, 171–186, 2009.
38. Siakavara, K. "Novel fractal antenna arrays of satellite networks: Circular ring Sierpinski carpet arrays optimized by genetic algorithms," *Progress In Electromagnetics Research*, Vol. 103, 115–138, 2010.
39. Obayashi, S. and S. Takanashi, "Genetic optimization of target pressure distributions for inverse design methods," *AIAA Journal*, Vol. 34, No. 5, 881–886, 1993.

40. Foster, N. F. and G. S. Dulikravich, "Three-dimensional aerodynamic shape optimization using genetic and gradient search algorithms," *Journal of Spacecraft Rockets*, Vol. 34, No. 1, 36–42, 1997.
41. Kumar, A., D. Sahoo, S. Chakraborty, and N. Chakraborty, "Gas injection in steelmaking vessels: Coupling a fluid dynamic analysis with a genetic algorithms-based pareto-optimality," *Materials and Manufacturing Processes*, Vol. 20, No. 3, 363–379, 2005.
42. Colaco, M. J. and G. S. Dulikravich, "Solidification of double-diffusive flows using thermo-magneto-hydrodynamics and optimization," *Materials and Manufacturing Processes*, Vol. 22, No. 5, 594–606, 2007.
43. Kumar, A., S. Chakraborty, and N. Chakraborty, "Fluid flow in a tundish optimized through Genetic Algorithms," *Steel Research International*, Vol. 78, No. 7, 517–521, 2007.
44. Davis, L., *Handbook of Genetic Algorithms*, Van Nostrand Reinhold, New-York, 1990.
45. Michalewicz, Z., *Genetic Algorithms + Data Structures = Evolution Programs*, Springer Verlag, 1992.